Materials Science in Semiconductor Processing ∎ (∎∎∎∎) ∎∎∎–∎∎∎

Contents lists available at ScienceDirect

Materials Science in Semiconductor Processing

journal homepage: www.elsevier.com/locate/mssp

Aging effects on the stability of nitrogen-doped and un-doped InGaZnO thin-film transistors

Jayapal Raja [a], Kyungsoo Jang [a], Nagarajan Balaji [b], Shahzada Qamar Hussain [b], S. Velumani [a,c], Somenath Chatterjee [d], Taeyong Kim [a], Junsin Yi [a,*]

[a] College of Information and Communication Engineering, Sungkyunkwan University, Suwon 440-746, Republic of Korea
[b] Department of Energy Science, Sungkyunkwan University, Suwon 440-746, Republic of Korea
[c] Department of Electrical Engineering (SEES), CINVESTAV-IPN, Col. San Pedro Zacatenco, Mexico City 07360, Mexico
[d] Department of Electronics and Communication Engineering, Sikkim Manipal Institute of Technology, Sikkim Manipal University, Sikkim 737136, India

ARTICLE INFO

Keywords:
Oxygen desorption
Shelf-life stability
InGaZnO
Moisture adsorption

ABSTRACT

The long-term electrical reliability/stability measurements, including negative bias stress and aging over 10 months of nitrogen-doped (N-doped) and un-doped amorphous InGaZnO thin-film transistors (a-IGZO TFTs) were investigated. Aged un-doped a-IGZO TFT exhibits larger threshold voltage shift (ΔV_{th}) of 2.43 V and turn on voltage shift (ΔV_{on}) of 5.37 V due to combination of the surface desorption of oxygen atoms and moisture adsorption. The noticeable decrease in ΔV_{th} (0.93 V) and ΔV_{on} (0.81 V) of in-situ nitrogen doped a-IGZO TFT indicates the surface interaction is prevented due to effective passivation of inactive oxygen's in the channel. After 10 months aging time, the ΔV_{th} (~2.66 V) and ΔV_{on} (~4.62 V) of un-doped devices were observed under the negative gate bias stress, which is comparable to ~0.83 V and ~0.85 V in nitrogen doped a-IGZO devices, respectively. The perspectives reported here shall be useful in fabricating passivation-free oxide based semiconductor TFTs for device operation in stable ambient conditions.

© 2015 Elsevier Ltd. All rights reserved.

1. Introduction

Amorphous oxide semiconductor (AOS) materials have shown their importance in TFTs application due to its high mobility (5–20 cm^2/V s), good uniformity and even low thermal budget [1,2]. The major advantage of AOS is that they can be deposited using conventional semiconductor process such as sputtering at room temperature (RT). These merits enhance the possibility of future electronic applications, such as active-matrix organic light-emitting-diode displays (AMOLEDs), flexible display and 3D display technologies. A variety of AOS have been studied including ZnO [3], InZnO [4], InGaZnO [1], etc., among these materials, amorphous InGaZnO (a-IGZO) is one of the most prominent candidates for channel layer in thin-film transistors (TFTs) [1,5]. Particularly, for AOS based TFTs work published till date, the staggered-bottom gate (SBG) structure dominates [6], due to ease of processing technique and enhanced electrical properties. Therefore, the back surface of the TFT's active layer (oxide materials) is easily interacting with ambient molecules [5,7], which leads to back-channel conduction paths in SBG type devices. Since Zn based oxide materials are well known as gas sensors and widely used in different sensing applications [8,9].

Additionally, the adsorption of water vapor [10] from the ambient atmosphere on the exposed channel layer and inactive oxygen atoms [11] within the channel layer are considered as the additional reasons on the degradation of the device reliability. In previous reports, passivation layers (such as SiN_x, SiO_x, Al_2O_3, TiO_x, etc.,) were deposited by using the sputtering or plasma enhanced chemical vapor

* Corresponding author. Tel.: +82 312907139.
E-mail address: yi@yurim.skku.ac.kr (J. Yi).

http://dx.doi.org/10.1016/j.mssp.2015.02.036
1369-8001/© 2015 Elsevier Ltd. All rights reserved.

ARTICLE IN PRESS

deposition system in vacuum. However, several research groups have reported that passivation layer placed on top of the air exposed back-channel surface of oxide TFTs is not compatible, thus causing shift in V_{th} to more negative voltages [12–14] due to O_2 removal from the surface as well as an increase in sub-threshold swing (SS) [13].

In this context, enormous effort has been performed toward the doping in Zn based oxide and/or high-*k* dielectric materials using various dopant elements (In, Li, Al, N, Mg, etc.,), which proves its utility in different applications, e.g. Shelke et al. showed that conductivity of ZnO may be enhanced by doping In, Al [15,16]. The Mg doped IGZO films were prepared by Wu et al. using the sputter deposition with 6.53 at.%. They have reported minimum carrier concentration of $9.18\times10^{17}/cm^3$ [17]. Su et al. reported that Li doped ZnO has a lower carrier concentration and oxygen deficiency than that of pure ZnO film [18]. Lim et al. revealed the carrier concentration, which was controlled to proper level by N doping in ZnO channel layer for the TFT devices [19]. Among those elements, N is theoretically suggested to be an excellent dopant in Zn based oxide materials due to its ionic radius and electro-negativity, which is close to O [20], and non-toxicity, which serve as defect binder. Chaudhuri et al. [21] reported that N incorporation in Gd_2O_3 dielectrics can reduce the leakage current conduction by effectively deactivating the oxygen vacancy (V_O) related gap states, which may enhance the dielectric reliability. Recently, Ahn et al. studied a solution based GaZTO:N TFT, which exhibited significantly improved positive bias stress induced instability compared to those of ZTO TFTs, because of a reduction in the oxygen-related defects located near the conduction band [22]. Generally, N-doping can be categorized into two types (i) direct doping during the formation of oxide/dielectric materials, which is called as "in-situ" doping; (ii) post-treatment of as-deposited oxide/dielectric materials with a nitrogen sources (NH_3, N_2, etc.), i.e., post-doping. An advantage of in-situ doping approach is that a more stable doping, less time consuming and easy process, which leads to improve the device properties of nitrogenated oxide based TFT devices.

However, the long-term aging stability and the device performance under the negative gate bias stability of N-doped a-IGZO TFTs have not been explored yet, which is one of the key problems that oxide based TFTs have to deal with when they are applied in the display industry. In this study, we present a time-dependent instability of the a-IGZO TFTs and the mechanism for the improvement in the shelf-life stability of N-doped a-IGZO TFT devices.

2. Experimental details

The SBG structure of N-doped and un-doped a-IGZO based TFT devices was fabricated in this work. A 100-nm-thick SiO_2 gate insulator film was deposited on n^{++} Si (100) wafers by inductively coupled plasma chemical vapor deposition (ICP-CVD) system with following parameters of power 200 W, pressure ~13.33 Pa, SiH_4/N_2O gas flow of 2/60 sccm. Before deposition of the active channel, the SiO_2/Si substrates were cleaned ultrasonically in acetone followed by iso-propyl alcohol for 10 min duration each, and next cleaned with de-ionized water and dried under N_2 gas.

A 100-nm-thick a-IGZO thin film was deposited at RT by DC magnetron sputtering using an IGZO ceramic target (4 in. diameter, atomic ratio In:Ga:Zn = 1:1:1, with 4 N purity) with the power density of 1.72 W/cm^2. The distance between the substrate and the target was fixed at 10 cm. Pre-sputtering was carried out for removing native contamination on the target surface. The carrier gas of Ar (20 sccm) and Ar + N_2 (20 + 0.3 sccm) was supplied into the chamber for depositing un-doped and N-doped a-IGZO thin films as an active channel layer, respectively, with the operating pressure of about 0.66 Pa. Subsequently, the samples were subjected to thermal annealing at 350 °C for 1 h duration in air ambient. After the 150-nm-thick silver source/drain (S/D) electrodes were deposited on top of the channel layer using a thermal evaporation technique. The active channel and S/D regions were patterned using photolithography and lift-off processes, respectively. The active channel width (*W*) and length (*L*) of our TFTs were 50 μm and 50 μm, respectively. The thickness of the SiO_2 and a-IGZO layers was measured using a spectroscopic ellipsometer (Model:MF-1000, Nano View). Additionally, the un-doped and N-doped a-IGZO single films were prepared in the same conditions (as mentioned above) with those for the fabrication of TFT devices to study their elemental analysis. The chemical compositions and oxygen vacancies of these films were observed using an X-ray photoelectron spectroscopy (XPS) (Model:ESCA 2000, VG Microtech) with an X-ray Al-Kα source.

All the electrical characterizations of the fabricated samples were conducted inside the black box using a probing station and a semiconductor parameter analyzer (EL420C). For aging stability study un-doped and N-doped films and their fabricated TFT devices were packed in lens cleaning paper and stored in normal atmosphere with a 50% relative humidity (RH). We recorded, the XPS analysis and electrical characterizations of TFT devices every five months, then ended in the 10th month periodically.

3. Results and discussion

The electrical properties of N-doped and un-doped a-IGZO devices were monitored during a period of 10 months. The transfer characteristics (with drain to source voltage of 1 V) and corresponding electrical parameters of these devices are shown in Fig. 1 and Table 1, respectively, with interval of 5 months. It is observed that the transfer curve shifts towards the left with the staying period in the atmosphere. This indicates that the conductivity of active channel was increased, due to generation of donor-like states. The extracted V_{th} and V_{on} of un-doped and N-doped a-IGZO TFTs with different aging periods are plotted in Fig. 2. Each error bar includes five different measured results to confirm reliability of each TFT device. As shown in Fig. 1(a) the V_{th} and V_{on} of un-doped a-IGZO TFT are increased apparently with the staying period. The value of V_{th} and V_{on} is shifted from 3.86 to 1.43 V and −1.76 to −7.13 V respectively, after 10 months stay at the ambient atmosphere under a RH of 50%. The possible origin of V_{th} instability in oxide based TFTs is easily occurs in the passivation-free back channel region and loosely bonded oxygen atoms in between metal networks of channel materials. In addition, we noted the slightly increasing trend

Please cite this article as: J. Raja, et al., Materials Science in Semiconductor Processing (2015), http://dx.doi.org/10.1016/j.mssp.2015.02.036

ARTICLE IN PRESS

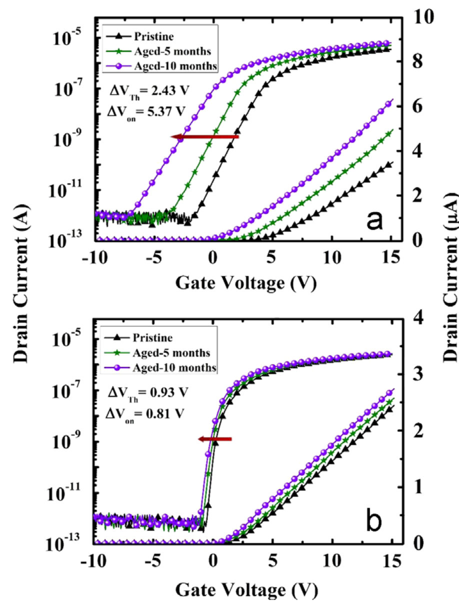

Fig. 1. Aging stability of (a) un-doped and (b) N-doped a-IGZO TFTs at different staying periods.

Table 1
Electrical parameters of un-doped and N-doped a-IGZO TFTs stayed at different aging periods, depicted in Fig. 1.

Devices	Δ=(Pristine ~aged 10 months)			
	ΔV_{th} (V)	ΔSS (V/dec)	ΔV_{on} (V)	ΔI_{on} (μA)
Un-doped	2.43	0.37	5.37	2.74
N-doped	0.93	0.06	0.81	0.91

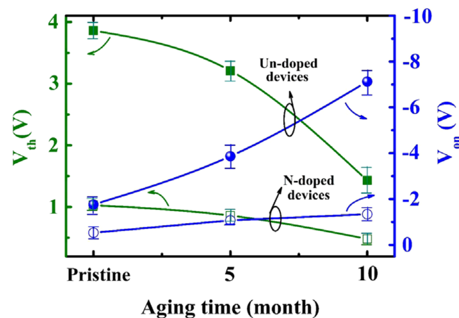

Fig. 2. The variation in the V_{th} and V_{on} values for un-doped and N-doped a-IGZO TFTs at different staying periods.

of SS, as observed in un-doped a-IGZO TFT during the aging time, which may be due to the creation of electron trap sites.

As in previous reports [10,23] on metal oxide based TFTs, moisture ($H_2O_{(g)}$) adsorption from the ambient atmosphere could form positively charged species ($H_2O^+_{(g)}$) in the surface of oxide film, which can be expressed in the form $H_2O^+_{(g)} \rightarrow H_2O^+_{(g)} + e^-$. During the aging period, absorbed moisture at the back surface of a-IGZO is donating more electrons in the channel, which causes the negative shift of V_{th}. Additionally, the inactive oxygen atoms from the IGZO backchannel region can react with the ambient atmosphere and causes a "desorption reaction" to form oxygen vacancies. The inactive oxygen atoms induces a turn on current shift (ΔI_{on}=2.74 μA) in un-doped devices during the aging periods. It can be also seen clearly that the V_{on} and V_{th} are different. These results are similar to those in the paper reported by Fuh et al. [11]. For the inactive oxygen, the oxygen desorption ($O_{2\ (des.)}$) reaction occurs continuously in the loosely bonded oxygen atoms between metal networks in the a-IGZO film, resultantly causing the additional reduction of V_{th} and V_{on} values with prolonged staying periods.

In contrast, N-doped a-IGZO TFT presents remarkable aging stability over time (see Fig. 1(b)). The value of V_{th} and V_{on} shifted from 1.03 to 0.10 V and −0.53 to −1.34 V respectively, after a same staying period in atmosphere. Furthermore, a small ΔI_{on} (0.91 μA) was observed in N-doped IGZO devices. These results indicated that the N atoms can partially replace the inactive loosely bound O atoms and reduce the $O_{2\ (des.)}$ reaction in the a-IGZO back channel. Additionally, the electron traps associated with V_O in the N-doped a-IGZO film were almost stable over the aging period, which is comparable with un-doped a-IGZO film. Moreover, the obtained results are confirmed from XPS studies (shown in Fig. 3). Deconvolution of the O 1s peak of these thin films showed the presence of three peaks centered at 530.01, 531.62, and 532.8 eV [17]. The calculated peak intensity ratios of these films are summarized in Table 2. The low binding energy peak (LP) centered at 530.01 eV related to O^{2-} ions surrounded by In, Ga and Zn atoms in the wurtzite IGZO structure. The middle binding peak (MP), centered at 531.6 eV was associated with O^{2-} ions in the oxygen-deficient regions within the IGZO matrix. The high binding peak (HP) at 532.8 eV is usually attributed to the presence of loosely bound oxygen impurities on the IGZO films, such as chemisorbed oxygen, oxygen interstitials or –OH groups.

As seen in Fig. 3(a)–(f), the intensity ratio of peak MP and HP is increased with aging period. The area ratios MP/(LP+MP+HP) in un-doped (N-doped) a-IGZO significantly increases from 16.27% (14.03%) for the pristine sample to 17.83% (14.51%) and 19.70% (14.97%) for the samples aged with 5 and 10 months, respectively. This indicates that the weakly bonded oxygen atoms were unstable in between metal networks, which could easily desorbed out of the surface of a-IGZO film and forming the V_O's providing extra free electrons in the channel [11]. In contrast, the $O_{2\ (des.)}$ effect was controlled with N-doped IGZO film, which prevents the devices aging failure. In addition, the ratio of HP/(LP+MP+HP) in a-IGZO film with un-doped and N-doped is 6.42% and 5.33%, 6.91% and 5.46%, 7.54% and 5.62% for the pristine, aged at 5 and 10 months, respectively, which shows excellent tolerance to moisture adsorption.

Also, we investigated the negative gate bias stress (NGBS) of these devices on different aging periods. When the negative gate bias (−20 V) was applied across the TFTs as stress voltage for duration of 5000 s, the donor like states (V_O related traps) is positively charged. This positively charged donor like states may be used to provide as providing more charge carriers for the conduction band of the a-IGZO device, showing the rapid increase of V_{th} and μ_{FE} during the NGBS. When applying the electrical stress, the loosely bound oxygen atoms (traps states) that could

Please cite this article as: J. Raja, et al., Materials Science in Semiconductor Processing (2015), http://dx.doi.org/10.1016/j.mssp.2015.02.036

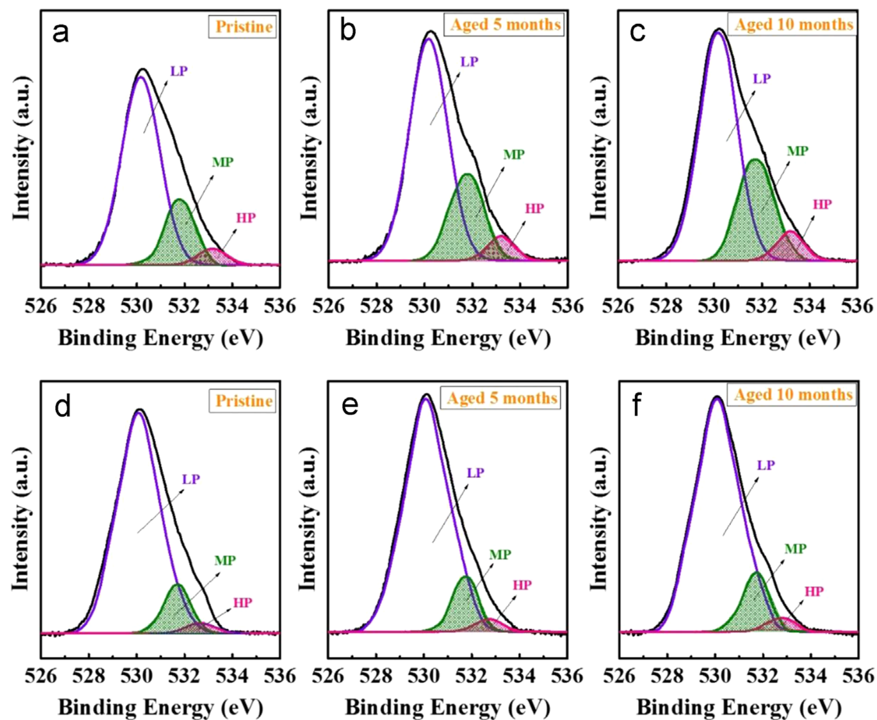

Fig. 3. O 1s region of XPS spectra measured for (a–c) un-doped (d–f) N-doped IGZO thin films with different staying periods.

Table 2
Summary of the peak intensity ratio of un-doped and N-doped IGZO samples stayed at different aging periods.

	Pristine		Aged 5 months		Aged 10 months	
	Un-doped	N-doped	Un-doped	N-doped	Un-doped	N-doped
MP/(LP+MP+HP)%	16.27	14.03	17.83	14.51	19.70	14.97
HP/(LP+MP+HP)%	6.42	5.33	6.91	5.46	7.54	5.62

move in the a-IGZO layer. During bias stress oxygen vacancies (V_O^{2+}; hole-trapping states) may have collected at the SiO_2 surface, resulting in additional $-V_{th}$ shift. Fig. 4 shows energy band diagram of un-doped and N-doped a-IGZO TFT devices under NGBS.

The total threshold voltage shift (ΔV_{th}) after 5000 s was merely 1.273 V and 0.457 V for the pristine state of un-doped and N-doped a-IGZO TFTs, respectively. The amount of ΔV_{th} corresponds to the number of captured electrons, which are also proportional to total number of trap states (interface trap states and the bulk trap states). The reduced ΔV_{th} is due to the incorporation of optimum value of nitrogen (flow of 0.3 sccm) in a-IGZO film. On the contrary, the positively charged donor states are less in the N-doped devices due to the suppression of oxygen vacancies and the interface trap states. The traps associated with activation energy ($E_a = E_C - E_F + \chi$, where E_c, E_F and χ are the energy at conduction band, energy at valance band and electron affinity, respectively) in the N-doped a-IGZO devices were reduced to ~0.61 eV, which is comparable to ~0.87 eV in un-doped a-IGZO devices. Additionally, the shrinking in band gap (E_g) energy (un-doped ~3.24 eV; N-doped ~3.18 eV) of N-doped a-IGZO channel

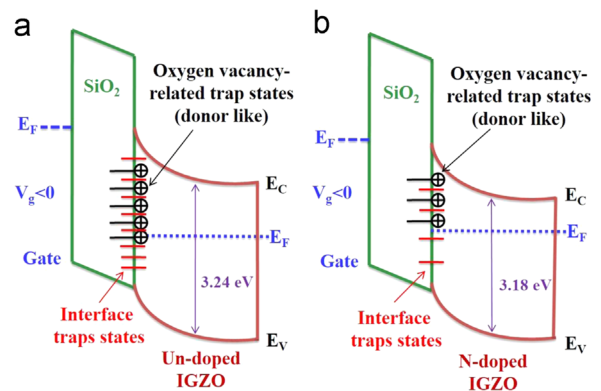

Fig. 4. Energy band gap diagram of (b) un-doped and (c) N-doped a-IGZO TFT devices under NGBS.

indicates the formation of Zn–N bonds [24] within a-IGZO matrix. The E_a and E_g are calculated from the Arrhenius plot using Ref. [25] and Tauc plot from UV–vis spectra, respectively (the calculation of E_g and E_a data are not shown).

Furthermore, it is clearly observed (from Figs. 5 and 6) that the values of ΔV_{th} and V_{on} of the 5 and 10 months aged N-doped a-IGZO TFTs during the NGBS study are all less than those of the un-doped a-IGZO devices. All the TFT devices (rest of Fig. 6(a)), a typical shift of transfer curves in the negative direction is observed due to hole-trapping. Conversely, the ΔV_{th} of the 10 months aged un-doped TFT device showed a turnaround behavior; the V_{th} shifted toward a negative side for stressing time of 2500 s and after that turned positive side. Cross et al. [26] suggest that the unstable V_{th} could have resulted from charge trapping

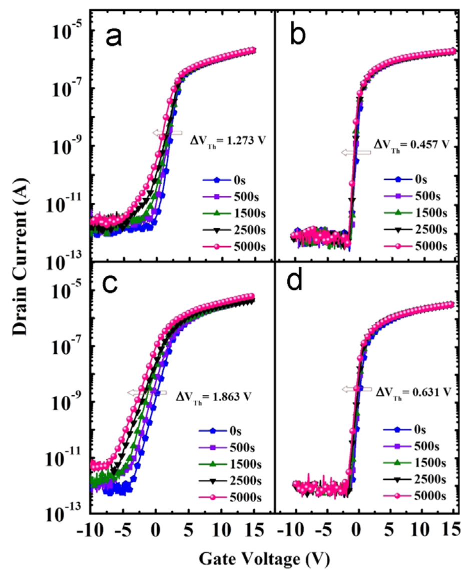

Fig. 5. Transfer characteristics of devices (a) un-doped; Pristine, (b) N-doped; Pristine, (c) un-doped; aged-5 months, and (d) N-doped; aged-5 months under NGBS.

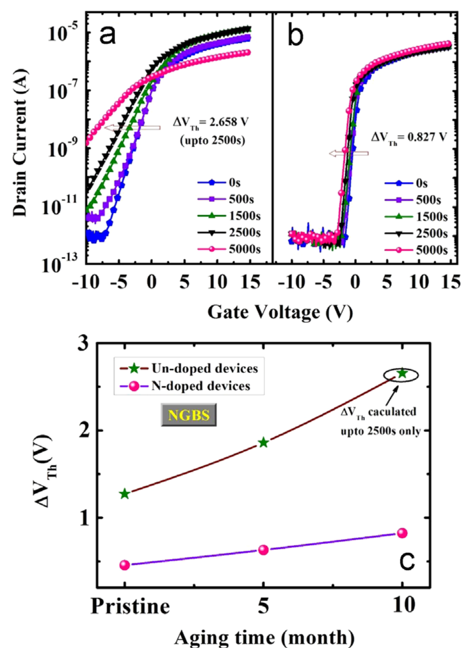

Fig. 6. Transfer characteristics of devices (a) un-doped; aged-10 months, (b) N-doped; aged-10 months, and (c) aging time variations of ΔV_{th} under NGBS for un-doped and N-doped a-IGZO devices.

competing with the defect generation. Conversely, the 10 months aged N-doped TFT device showed a reduction of ΔV_{th} to 0.827 V, which is compared to 2.658 V (predicted upto 2500 s, because of 5000 s stressed curve shift on positive side) in the 10 months aged un-doped a-IGZO devices. Additionally, the ΔV_{on} of N-doped devices are very small. The extracted ΔV_{th} values of these devices were plotted in Fig. 6(c). The instability of un-doped a-IGZO devices, the $O_{2\,(des.)}$ occurs continuously in the back channel surface and form oxygen vacancies in the a-IGZO channel, causing the reduction of V_{th} values for prolonged durations.

The nitrogen doped a-IGZO TFTs showed superior resistant against long-term aging compared with those of a un-doped a-IGZO TFT, which is a useful (in-situ) passivation technique for future amorphous-oxide semiconductor based thin-film transistors.

4. Conclusion

The long-term aging stability of the sputtered un-doped and N-doped a-IGZO TFTs over 10 months was investigated. The N-doped a-IGZO TFTs hindered the desorption of oxygen and moisture adsorption on the N-doped a-IGZO layer by effective passivation. Under negative bias stress, the N-doped devices showed a V_{th} shift (~0.83 V) and V_{on} shift (~0.85 V) compared to ~2.66 V and ~4.62 V in un-doped devices, respectively. Thus the in-situ nitrogen doping is a proper passivation method to prevent the interaction of inactive oxygen atoms in atmosphere for long-term reliability aspects of oxide based thin-film transistors.

Acknowledgments

This work was supported by the Basic Science Research Program through the National Research Foundation of Korea (NRF) funded by the Ministry of Education (NRF-2010–0020210) and by the Human Resources Development Program (No. 20124010203280) of the Korea Institute of Energy Technology Evaluation and Planning (KETEP) Grant funded by the Korea Government Ministry of Trade, Industry and Energy.

References

[1] T. Kamiya, K. Nomura, H. Hosono, Sci. Technol. Adv. Mater. 11 (2010) 044305.
[2] J. Raja, K. Jang, et al., IEEE Electron Device Lett. 35 (2014) 756.
[3] E. Fortunato, P. Barquinha, A. Pimentel, A. Gonsalves, A. Marques, L. Pereira, R. Martins, Adv. Mater. 17 (2005) 590.
[4] J.I. Song, J.S. Park, H. Kim, et al., Appl. Phys. Lett. 90 (2007) 022106.
[5] J.H. Jeong, H.W. Yang, J.-S. Park, J.K. Jeong, Y.-G. Mo, H.D. Kim, J. Song, C.S. Hwang, Electrochem. Solid-State Lett. 11 (2008) H157.
[6] E. Fortunato, P. Barquinha, R. Martins, Adv. Mater. 24 (2012) 2945.
[7] D. Kang, H. Lim, C. Kim, I. Song, J. Park, Y. Park, J. Chung, Appl. Phys. Lett. 90 (2007) 192101.
[8] A. Wei, L. Pan, W. Huang, Mater. Sci. Eng. B 176 (2011) 1409.
[9] H.S. Moon, S.E. Kim, W.C. Choi, Trans. Electr. Electron. Mater. 13 (2012) 106.
[10] C.S. Fuh, S.M. Sze, P.T. Liu, L.F. Teng, Y.T. Chou, Thin Solid Films 520 (2011) 1489.
[11] C.S. Fuh, P.T. Liu, Y.T. Chou, L.F. Teng, S.M. Sze, ECS J. Solid State Sci. Technol. 2 (2013) Q1.
[12] D. Hong, J.F. Wager, J. Vac. Sci. Technol. B, Microelectron. Nanometer Struct. 23 (2005) L25.
[13] D.A. Mourey, D.A. Zhao, J. Sun, T.N. Jackson, IEEE Trans. Electron Devices 57 (2010) 530.
[14] T.C. Chen, T.C. Chang, T.Y. Hsieh, et al., Appl. Phy. Lett. 97 (2010) 192103.
[15] V. Shelke, M.P. Bhole, D.S. Patil, Mater. Chem. Phys. 141 (2013) 81.
[16] V. Shelke, M.P. Bhole, D.S. Patil, J. Alloy. Compd. 560 (2013) 147.
[17] H.C. Wu, T.S. Liu, C.H. Chien, ECS J. Solid State Sci. Technol. 3 (2014) Q24.
[18] B.Y. Su, S.Y. Chu, Y.D. Juang, IEEE Electron Device Lett. 59 (2012) 700.
[19] S.J. Lim, S.J. Kwon, H. Kim, Appl. Phy. Lett. 91 (2007) 183517.
[20] L. Liu, J. Xu, D. Wang, M. Jiang, et al., Phys. Rev. Lett. 108 (2012) 215501.

ARTICLE IN PRESS

[21] A.R. Chaudhuri, A. Fissel, V.R. Archakam, H.J. Osten, Appl. Phy. Lett. 102 (2013) 022904.
[22] B.D. Ahn, H.J. Jeon, J.S. Park, ACS Appl. Mater. Interfaces 6 (2014) 9228.
[23] J.K. Jeong, H.W. Yang, J.H. Jeong, Y.G. Mo, H.D. Kim, Appl. Phys. Lett. 93 (2008) 123508.
[24] M. Futsuhara, K. Yoshioka, O. Takai, Thin Solid Films 317 (1998) 322.
[25] C.J. Ku, Z. Duan, P.I. Reyes, Y. Lu, Y. Xu, C.L. Hsueh, E. Garfunkel, Appl. Phys. Lett. 98 (2011) 123511.
[26] R.B.M. Cross, M.M. De Souza, Appl. Phys. Lett. 89 (2006) 263513.

Please cite this article as: J. Raja, et al., Materials Science in Semiconductor Processing (2015), http://dx.doi.org/10.1016/j.mssp.2015.02.036